GPC Analysis of Polymer Network Formation: 1. Bifunctional Siloxane Monomer/Crosslinker System

Shinzo Kohjiya,* Yasuhiro Takada, Kenji Urayama, Yasuyuki Tezuka,† and Akinori Kidera††

Institute for Chemical Research, Kyoto University, Uji, Kyoto 611

†Department of Organic and Polymeric Materials, Tokyo Institute of Technology, O-okayama, Meguro-ku, Tokyo 152

††Biomolecular Engineering Research Institute, Suita, Osaka 565

(Received September 8, 1995)

The size distribution of polymer clusters in the pre-gel state was investigated as a function of the conversion by gel permeation chromatography (GPC) in order to elucidate the process of polysiloxane network formation. Polysiloxane networks were synthesized by hydrosilylation between a bifunctional monomer and a tri- or tetrafunctional crosslinker. Experimental chromatograms for the pre-gel system were compared with a theoretical one based on the distribution for the mean-square radius of gyration ($\langle S^2 \rangle$) of polymer clusters predicted by the Flory–Stockmayer theory and the Gaussian chain statistics. Experimental chromatograms at high conversion showed a longer tailed distribution in the large $\langle S^2 \rangle$ region compared with a theoretical one. A comparison of experimental chromatograms with theoretical ones suggests the structure of a precursor network in which branched clusters are linearly linked.

Studies on the formation of polymer networks have been both experimentally and theoretically performed by many researchers. The behavior of molecular size[1—3] and viscoelasticity[4—6] near to the gelation point has been investigated for various gel systems. The evolution of the network structure in the pre-gel state has been interpreted in terms of an increase in the weight-average molecular weight (M_w) and the z-average mean-square radius of gyration ($\langle S^2 \rangle_z$). However, it is well known that the pre-gel system has a broad distribution of molecular sizes. Measurements of the distribution, itself, as well as the mean values should be indispensable for elucidating the formation process of polymer gel. In this study we investigated the size distribution for polysiloxane networks in the pre-gel state as a function of the conversion by gel permeation chromatography (GPC). (GPC is also called size exclusion chromatography (SEC).)

The classical theory[7—9] proposed by Flory and Stockmayer, or the percolation theory,[10—12] are often employed for theoretical interpretations of the gel-formation mechanism. The Flory–Stockmayer model, based on Bethe lattice, gives an analytical solution for the molecular-weight distribution at a certain degree of conversion, while the percolation model on a finite-dimensional lattice does not. However, it is not possible for branched polymer clusters that GPC traces is to be directly related to the molecular weight distribution, because the chromatograms are governed by the $\langle S^2 \rangle$ distribution of polymer clusters. Schosseler et al.[13] reported on the size distribution of polystyrene clusters in the pre-gel state by GPC coupled with light scattering. They related the theoretical molecular weight distribution to the experimental chromatograms by employing a semiempirical calibration law representing the relationship for the elution volume between linear and branched molecules. In our previous paper[14] we evaluated the $\langle S^2 \rangle$ distribution of polymer clusters in the pre-gel state as a function of the conversion by a computer simulation on the basis of the Flory–Stockmayer model[7—9] and the Gaussian chain statistics.[15,16] By exhausive enumeration using iteration equations, all of the species of the clusters in the pre-gel system were counted one by one, and the weight fraction and $\langle S^2 \rangle$ for each cluster were calculated. As expected, the calculated $\langle S^2 \rangle$ distribution was different from the theoretical molecular weight distribution, due to the fact that molecules with identical molecular weight can have various topological structures. In this study we compared the experimental chromatograms with theoretical ones calculated from the $\langle S^2 \rangle$ distribution obtained by the computer simulation mentioned above.

Polysiloxane networks are often used as a "model network" in studies of rubber elasticity. The networks are synthesized by the hydrosilylation between bifunctional poly(dimethylsiloxane) as a prepolymer and multifunctional silane as a crosslinker. Although there have been numerous studies on the mechanical properties of polysiloxane networks,[17—21] those on the reaction (gelation) and structure have been quite few,[22,23] despite their importance in using polysiloxane networks as a model network to simulate the theoretical elasticity. In this study, in order to investigate the effect of the synthetic conditions on gel formation, the size distribution in the pre-gel state was examined while varing the functionality of the crosslinker, reaction temperature, catalyst concentration, monomer concentration, and molar ratio of the crosslinker to the monomer. Finally, we discuss the mechanism of gel formation and deduce the post-gel structure based on a comparison of the experimental results on

the pre-gel with a theoretical prediction.

Experimental

Materials. 1,4-Phenylene-1,1′-bis(1,1,3,3-tetramethyl-3-vinyldisiloxane) (VT-M) $C_6H_4[Si(CH_3)_2OSi(CH_3)_2CH{=}CH_2]_2$ and 1,4-phenylene-1,1′-bis(1,1,3,3-tetramethyldisiloxane) (HT-M) $C_6H_4[Si(CH_3)_2OSi(CH_3)_2H]_2$ were used as bifunctional monomers. The synthesis of VT-M has been described elsewhere.[23,24] HT-M was newly synthesized in this study. HT-M was prepared by the same procedure as that for VT-M, except for using dimethylchlorosilane (purchased from Chisso Co.) instead of the dimethylvinylchlorosilane used in preparing VT-M. Dimethylvinylchlorosilane was distilled over CaH_2. The molecular weight of synthesized VT-M and HT-M was estimated by mass spectroscopy to be, respectively, 394.5 and 342.0, which agree well with those calculated from the chemical formula. The functionality of VT-M and HT-M was found to be, respectively, 1.98 and 1.90 by ^{1}H NMR, which are close to 2.

Methyltris(dimethylsiloxy)silane (F3-C) $CH_3Si[OSi(CH_3)_2H]_3$, phenyltris(dimethylsiloxy)silane (PF3-C) $C_6H_5Si[OSi(CH_3)_2H]_3$, and tetrakis(dimethylsiloxy)silane (F4-C) $Si[OSi(CH_3)_2H]_4$ were employed as tri- and tetrafunctional crosslinker, respectively. F3-C, PF3-C and F4-C were purchased from Chisso Co. and were used without further refinement.

$H_2PtCl_6{\cdot}6H_2O$ dissolved in 2-propanol (Speier's catalyst) was used as a catalyst for hydrosilylation.[25,26] The solvent for hydrosilylation was the toluene obtained by distilling the commercial one over Na wire.

Hydrosilylation Procedure. Tri- and tetrafunctional crosslinker (F3-C, PF3-C, and F4-C, respectively), or bifunctional monomer (HT-M) was mixed with VT-M at a certain ratio. The hydrosilylation reaction was carried out in the bulk state or in solution with 0.05 or 0.20 g ml^{-1} for the monomer concentration. The mixture was kept at a certain temperature in an oil bath, and a catalyst was added. After the solution was extracted from the reaction bath at a certain degree of conversion, toluene was removed. The extractive was dissolved in trichloromethane to 4.4 g l^{-1} for GPC, and in deuterated trichloromethane ($CDCl_3$) to 0.05 g ml^{-1} for ^{1}H NMR. We performed the hydrosilylation reaction under various conditions, as shown in Table 1: functionality of the crosslinker, the molar ratio of the silane hydrogen in the crosslinker to the vinyl group in the monomer (r), the monomer concentration (c), the catalyst concentration, and the reaction temperature (T) were varied. The effect of the synthetic conditions on the size distribution was investigated mainly for the hydrosilylation between VT-M and F4-C.

Table 1. Reaction Conditions for Hydrosilylation

Sample	r	c / g ml^{-1}	[Cat.]/[Si–H] $\times 10^5$/(mol/mol)	T / °C
F4-1	1.0	0.05	0.2	50
F4-2	1.0	0.05	0.2	75
F4-3	1.0	0.05	0.2	100
F4-4	1.0	0.05	1.0	50
F4-5	1.0	0.2	0.2	50
F4-6	1.0	Bulk	0.02	50
F4-7	0.6	0.05	0.2	50
F4-8	1.5	0.05	0.2	50
F3-1	1.0	0.05	0.2	50
PF3-1	1.0	Bulk	0.2	80
F2-1	1.0	Bulk	0.12	50
F2-2	2.1	Bulk	0.12	50

Determination of the Degree of Conversion. The degree of conversion (p) was determined by a ^{1}H NMR analysis. The value of p was determined in terms of the conversion of the vinyl group and/or silane hydrogen in many studies.[17,18] It is well-known,[27,28] however, that the hydrosilylation reaction consists of α and β additions, and is accompanied by a side reaction, such as hydrogenation to vinyl groups (see Scheme 1 for details). Accordingly, we evaluated the respective amount of α, β addition and hydrogenation by ^{1}H NMR, and determined p to be the sum of α and β additions. The following is the determination procedure of p. As an example, the ^{1}H NMR spectrum of F4-6 at $p = 0.455$ is presented in Fig. 1. The signals related to the procedure are assigned as follows: Signal d to the protons of the methylene group created by β addition, f to the methyl group by α addition, and j to the methyl group by hydrogenation. The number of protons of the vinyl groups consumed on α and β addition (V_α and V_β, respectively) was obtained as $V_\alpha = M_\alpha$ and $V_\beta = (3/4)M_\beta$. Here, M_α and M_β are the number of protons assigned to signals f and d, respectively. The number of protons in vinyl groups before the reaction (V_0) is given by $V_0 = (3/2)B$, where B is the number of protons in benzene rings. The value of p is obtained as the sum of the degree of α addition (V_α/V_0) and that of β addition (V_β/V_0):

$$p = \frac{V_\alpha + V_\beta}{V_0}. \quad (1)$$

The degree of hydrogenation was evaluated using the same procedure, and the number of protons assigned to signal j.

Apparatus. Chromatograms were obtained with a Shimadzu GPC LC-6A equipped with Shimpack GPC-8025, 804 and 801 columns. The column temperature was 40 °C, and the flow rate was 1.0 ml min^{-1}. The polymer concentration of the elute was detected by UV absorption with a Shimadzu MPS-2000. ^{1}H NMR spectra were acquired with a Hitachi NMR R1000 ^{1}H NMR spectrometer and a GE QE300 ^{1}H NMR spectrometer using $CDCl_3$ as a solvent. The mass spectra were obtained with a Hitachi M-80B.

Calculation Methods for Theoretical GPC Traces

We simulated the $\langle S^2 \rangle$ distribution of (i,j)mer, which consists of i and j pieces of a crosslinker and a monomer, respectively, as a function of the conversion on the basis of the Flory–Stockmayer model and Gaussian chain statistics. The details concerning the simulation were described in our previous paper.[14] In order to exclude the complexity in the size determination for the clusters, the number of monomers

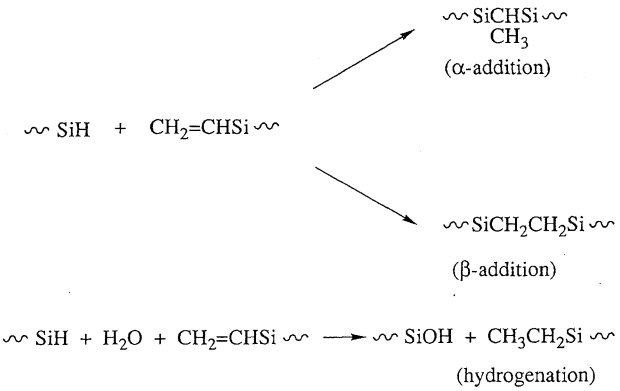

Scheme 1.

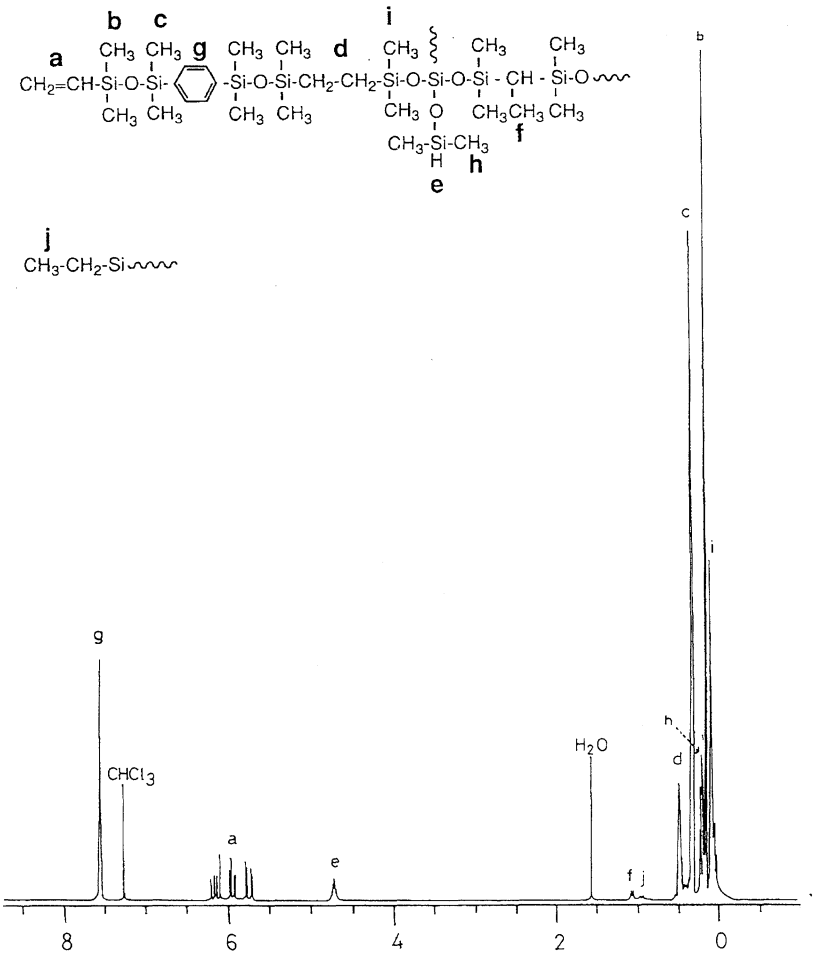

Fig. 1. ^{1}H NMR spectrum of F4-6 at $p = 0.455$ with the signal assignment.

(i) in (i, j)mer was converted into a number whose unit is a crosslinker (x). The size of (i, j)mer was considered to be equal to that of a cluster comprising $(x+j)$ pieces of the crosslinker. Here, the size ratio of the monomer to the crosslinker was approximated by the molecular weight ratio. This simplification is valid in the case that the monomer and crosslinker have similar molecular structures. In the case of this study, the simplification is assumed to be valid based on the chemical structure of the monomer and the crosslinker used here.

For a comparison with experimental GPC traces, we calculated theoretical ones based on simulation results for the $\langle S^2 \rangle$ distribution (as described below). Since the chromatogram, even for a monodisperse polymer, has a peak with a width, the theoretical GPC trace for a multidisperse system should comprise peaks with a width corresponding to each monodisperse $\langle S^2 \rangle$ fraction. The chromatogram $(F(v))$ of a monodisperse polymer can be expressed by a Gaussian function,[29]

$$F(v) = A\sqrt{\frac{k^2}{\pi}} \exp\left[-k^2(v - v_0)^2\right], \tag{2}$$

where A is the area of the chromatogram, k the quantity related to the inverse of the half width of the peak, v the elution volume, and v_0 the value of v at the maximum of the peak. In the case of a polydisperse polymer, $F(v)$ is given by the sum of chromatograms of monodisperse polymer fractions, as follows:[29]

$$F(v) = \sum_i A_i \sqrt{\frac{k_i^2}{\pi}} \exp\left[-k_i^2(v - v_{0,i})^2\right]. \tag{3}$$

We calculated the theoretical GPC traces using Eq. 3, where the value of k_i was determined based on the half width of the peak of VT-M. The values of k_i in low and high elution volume sides were separately determined using the half width in the respective sides, taking the unsymmetry of experimental peak into account.

The polymer concentration of the elute was experimentally detected by the UV in this study. The monomers and crosslinkers used in this study were different in sensitivity to UV. Accordingly, we calculated the intensity of the theoretical chromatogram at p while considering the difference in intensity between the monomer and crosslinker, which could be estimated from the respective peaks in the experimental chromatogram at p=0.

Results

α-, β-Additions and Hydrogenation in Hydrosilylation

Reaction. The results for hydrosilylation between VT-M and F4-C under various synthetic conditions and at various degrees of conversion are given in Table 2. F4-6, prepared by bulk polymerization, indicated a smaller degree of hydrogenation compared with samples produced by solution polymerization.

Hydrosilylation between Bifunctional Monomer and Tetrafunctional Crosslinker. Figure 2 shows the change in M_w/M_n with conversion for hydrosilylation between VT-M and F4-C, where M_n is the number-average molecular weight. The theoretical values by the Flory–Stockmayer model are also shown in the figure. The broken line in the figure corresponds to the gel point (p=0.58) predicted by Flory–Stockmayer theory. The values of M_w/M_n for F4-1, -2, -3, -4, and -5, prepared by solution polymerization, which overlap in the figure, were almost identical irrespective of the differences in the other reaction conditions, and were slightly larger than the theoretical value. The values for F4-6, prepared by bulk polymerization, were larger than those for samples by solution polymerization and theoretical ones; the difference became greater with increasing conversion.

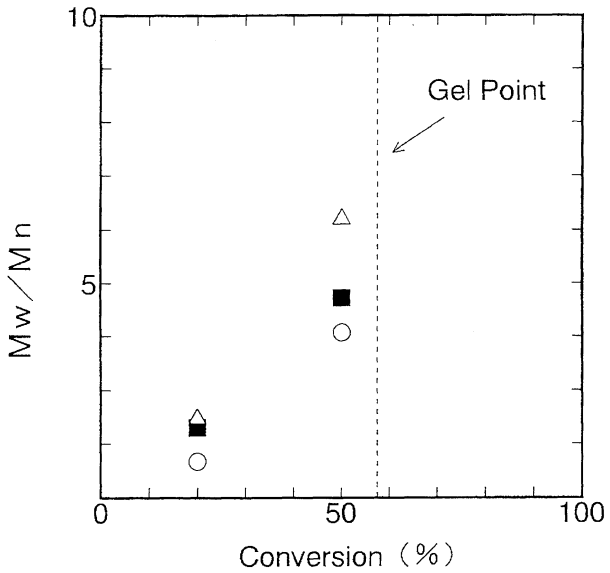

Fig. 2. Change of M_w/M_n with conversion for the hydrosilylation between VT-M and F4. Symbols: calculated (○); experimental (△) F4-6, (■) F4-1, -2, -3, -4, and -5.

At low conversion ($p<0.25$), the chromatograms of all samples with r=1 (F4-1—F4-6) were almost identical, and did not have any significant dependences on the reaction conditions. As an example, the chromatograms of F4-1 at p=0.244 and F4-2 at p=0.210, prepared at different reaction temperatures, are shown in Fig. 3a. The quantity at the vertical axis is related to the response to UV, and that at the horizontal axis is proportional to the logarithm of $\langle S^2 \rangle$ and the inverse of the elution volume of molecules. Both quantities have arbitrary units. The location of the peak corresponding to the crosslinker is set at the zero of the horizontal axis. In Fig. 3a, since the peak intensity for the monomer (VT-M) having a benzene ring sensitive to UV is much stronger than that for the crosslinker (F4-C), the peak assigned to F4-C is covered with that to VT-M. As can be seen in Fig. 3a, the reaction temperature does not have any considerable influence on the size distribution. Figure 3b

Table 2. Data for the Degree of α, β Additions and Hydrogenation in the Hydrosilylation between VT-M and F4

Sample	Reaction time (h)	α (%)	β (%)	Hydrogenation (%)	p	α/β
F4-1	1.00	0.8	5.0	0.8	5.8	0.16
	8.00	2.9	19.8	1.1	22.4	0.15
	20.00	4.5	33.7	2.3	38.2	0.13
F4-2	0.08	0.8	8.6	0.8	9.4	0.09
	0.25	2.3	18.7	0.8	21.0	0.12
	1.00	4.9	43.9	2.4	48.8	0.11
F4-3	0.08	2.6	20.3	0.8	22.9	0.13
	0.25	3.5	33.0	1.4	36.5	0.11
	0.50	3.8	44.4	1.9	48.2	0.09
F4-4	0.08	3.3	19.4	0	22.7	0.17
	0.50	5.7	30.7	1.9	36.4	0.19
	4.00	5.3	44.9	2.7	50.2	0.15
F4-5	1.00	1.9	15.3	0	17.2	0.12
	8.00	5.8	33.8	1.3	39.6	0.17
	16.00	5.8	38.1	1.7	43.9	0.15
F4-6	0.25	2.9	16.5	0	19.4	0.18
	1.00	5.1	28.8	0.2	33.9	0.18
	2.50	5.8	39.7	0.5	45.5	0.15
F4-7	10.00	2.7	22.3	1.3	25.0	0.12
	20.00	4.0	28.8	2.7	32.8	0.14
	30.00	5.3	33.2	2.7	38.5	0.16
F4-8	3.00	1.1	6.7	0.5	7.8	0.16
	6.00	2.9	18.4	1.2	21.3	0.16
	40.00	4.4	30.5	2.9	34.9	0.14

shows a comparison of the chromatogram of F4-1 at p= 0.224 with the theoretical one. The theoretical curve agrees well with the experimental one. The horizontal scale of the theoretical curve was determined so that the peak of the monomer, which is located at 0.2 count, can coincide with that for the experimental chromatogram.

The synthetic conditions, such as the reaction temperature and catalyst concentration, did not have any remarkable effect on the size distribution at high conversion or at low conversion. The chromatograms of F4-1, -2, -3, -4, and -5 at high conversion were almost identical, although their chromatograms are not presented here. However, the chromatograms at high conversion depended on the monomer concentration. The GPC traces of F4-4 at p=0.502 and F4-6 at p=0.455, which were respectively prepared by solution and bulk polymerization, are presented in Figs. 4a and 4b. The theoretical traces are also shown in the figures. Two significant differences between the experimental and theoretical traces can be seen in Fig. 4a: (1) the peak assigned to the dimer, which is located at about 0.8 in the theoretical trace, is shifted to the left in the experimental one; (2) the experimental distribution has the longer tail in the large $\langle S^2 \rangle$ region, while the peak located at about 1.8 in the theoretical curve is not seen in the experimental one. On the other hand, the peaks of the dimer in both curves coincide in Fig. 4b. The discrepancy in the large $\langle S^2 \rangle$ region is almost identical with that in Fig. 4a.

The chromatograms of F4-7 at p=0.385 and F4-8 at p=

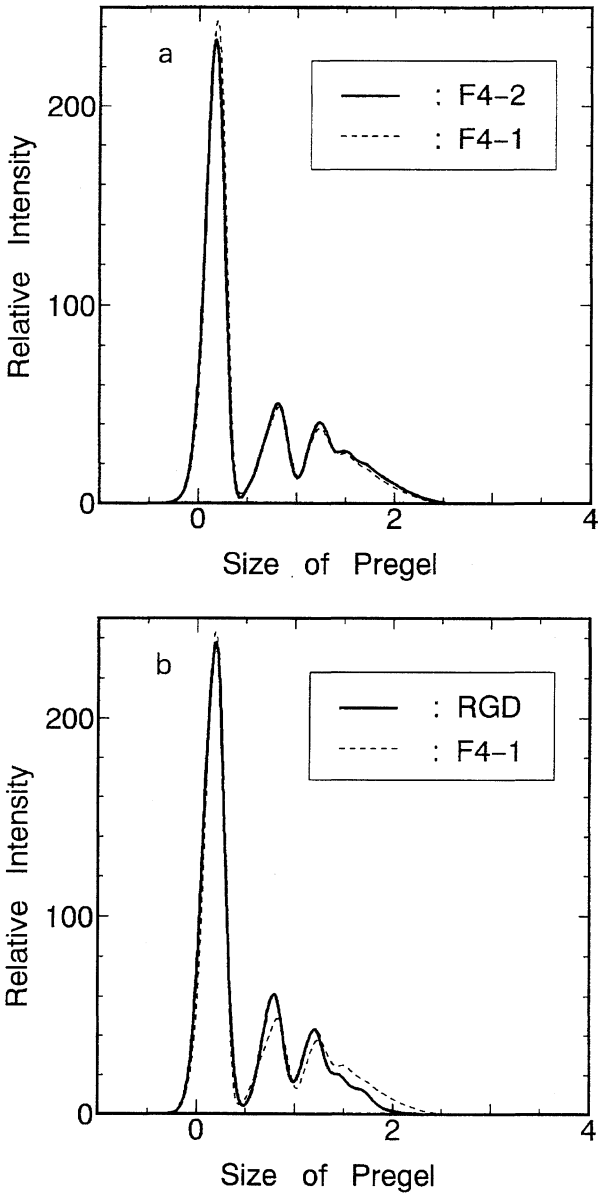

Fig. 3. (a) Comparison of the GPC curves of F4-1 at p=0.224 and F4-2 at p=0.210. (b) Comparison of the GPC curve of F4-1 at p=0.224 with the calculated curve (RGD).

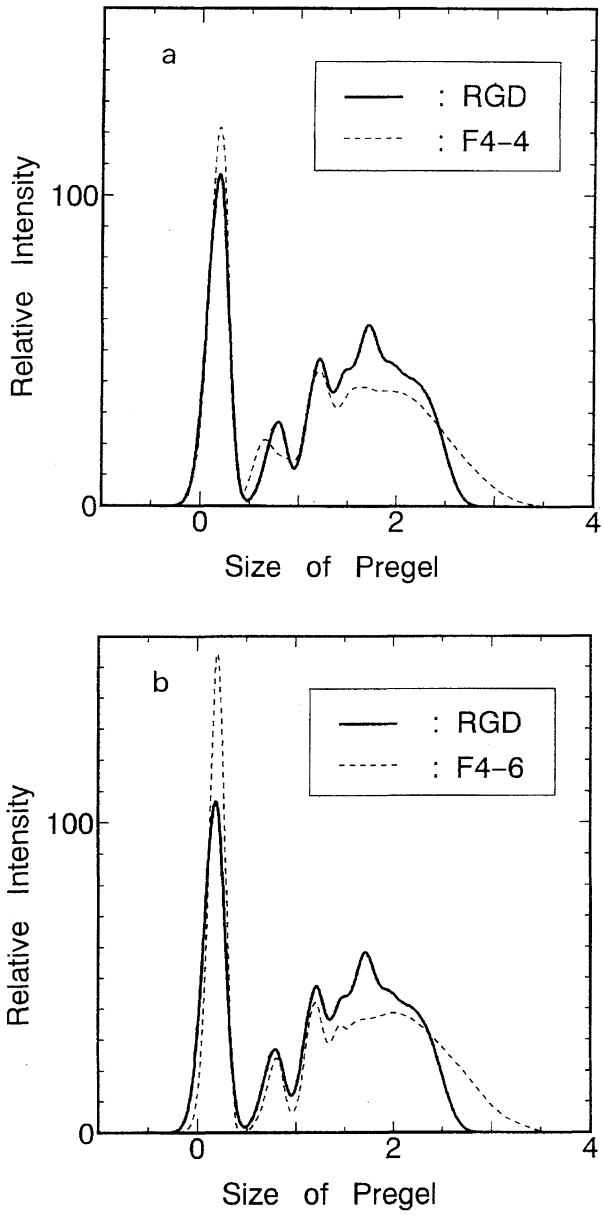

Fig. 4. (a) Comparison of the GPC curve of F4-4 at p=0.502 with the theoretical curve (RGD). (b) Comparison of the GPC curve of F4-6 at p=0.455 with the calculated curve (RGD).

0.349, which were respectively prepared at $r=0.6$ and $r=1.5$, are presented in Figs. 5a and 5b, respectively. The theoretical curves are also shown in the figures. Although the dependences of the size distribution on the r value are observed, the features in a comparison of the experimental traces with the theoretical ones are similar to those for those samples with $r=1$.

Hydrosilylation between Bifunctional Monomer and Trifunctional Crosslinker. The GPC traces of F3-1 at $p=0.437$ and PF3-1 at $p=0.500$, which were respectively prepared by solution and bulk polymerization, are shown along with the theoretical ones in Figs. 6a and 6b. The differences between the experimental curves and the theoretical ones for F3-1 and PF3-1 are similar to those for F4-4 prepared by solution polymerization and those for F4-6 by bulk polymerization, respectively. It can be seen in Fig. 6b that the peaks assigned to the unreacted monomer and crosslinker, which are respectively located at 0.2 and 0, are different in the intensity between the experiment and the theory: The experimental quantity of monomer is greater, and that of crosslinker is smaller compared with theoretical ones. It should be noted that PF-3C with a benzene ring is sensitive to UV compared with F4-C and F3-C, which explains why the peak assigned to PF3-C is clearly seen in Fig. 6b, while that to F4-C and F3-C is not noticeable in Figs. 3, 4, and 5. The different shape of the trace for PF3-1 from those for

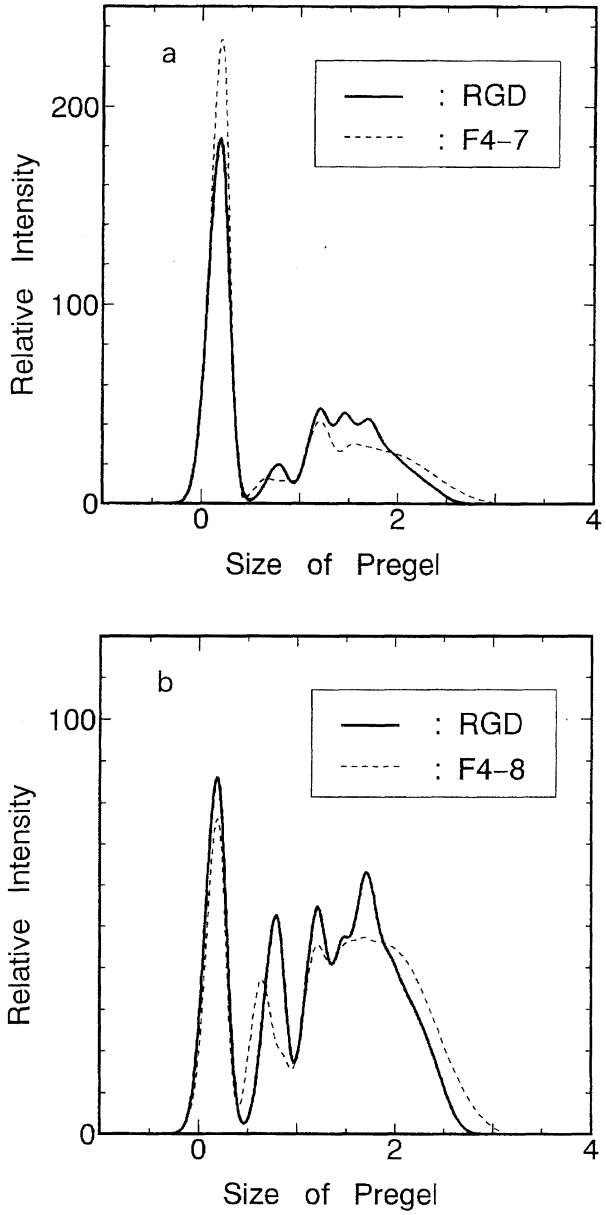

Fig. 5. (a) Comparison of the GPC curve of F4-7 at $p=0.385$ with the calculated curve (RGD). (b) Comparison of the GPC curve of F4-8 at $p=0.349$ with the calculated curve (RGD).

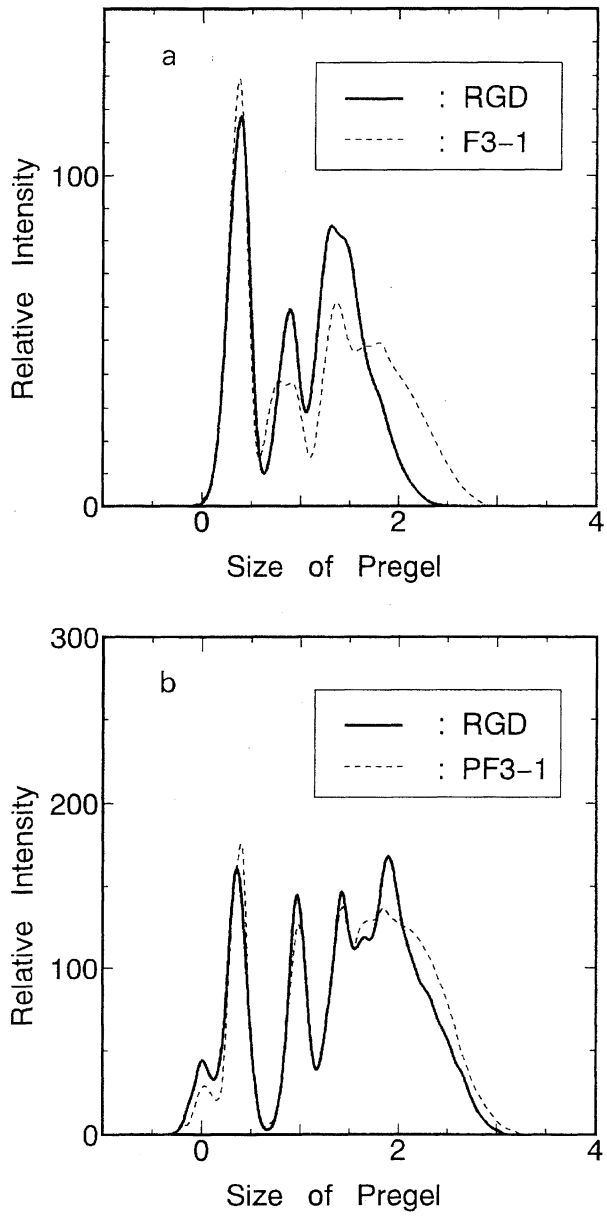

Fig. 6. (a) Comparison of the GPC curve of F3-1 at $p=0.437$ with the theoretical curve (RGD). (b) Comparison of the GPC curve of PF3-1 at $p=0.500$ with the calculated curve (RGD).

other samples at $p \approx 0.5$ is explained by the same reason.

Hydrosilylation between Bifunctional Monomers. Figures 7a and 7b indicate the chromatograms of F2-1 at p=0.65 and F2-2 at p=0.70, which were prepared at r=1 and r=2.1, respectively. The theoretical curves are also presented in the figures. The size distribution in the large $\langle S^2 \rangle$ region for F2-1 is shifted to the low $\langle S^2 \rangle$ side compared with the theoretical distribution. The GPC trace of F2-2 is well reproduced by the theoretical one. The peak assigned to HT-M almost coincides with that to VT-M, because the molecular size is comparable to that of VT-M.

Discussion

α, β Additions and Hydrogenation in Hydrosilylation

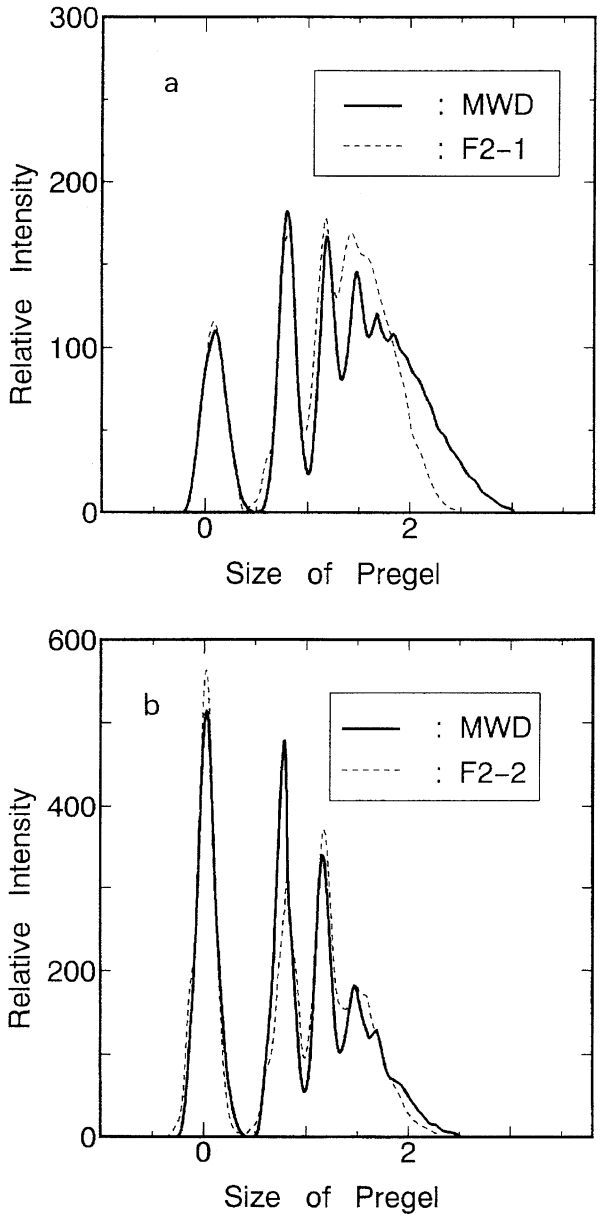

Fig. 7. (a) Comparison of the GPC curve of F2-1 at p=0.650 with the calculated curve (RGD). (b) Comparison of the GPC curve of F2-2 at p=0.700 with calculated curve (RGD).

Reaction. It can be seen in Table 2 that β addition is the dominant reaction in the hydrosilylation for all samples, and the contribution of α addition is minor. The contribution of hydrogenation to the total reaction was estimated to be less than 5% for all samples, suggesting that the effect of hydrogenation on the crosslinking reaction is negligible in this study. The smaller amount of hydrogenation in bulk polymerization (F4-6) should be due to the smaller quantity of protons in the system; a very small amount of adventitious water in toluene used in solution polymerization contributed to the hydrogenation.

Hydrosilylation between Bifunctional Monomer and Tetrafunctional Crosslinker. The value of M_w/M_n and the experimental chromatograms at low conversion were well-described by theory, regardless of the details concerning the reaction conditions, as shown in Figs. 2 and 3. This result suggests that the system at low conversion has a tree-like structure, as predicted by theory. On the other hand, at high conversion, discrepancies between the theory and the experiment appeared in the value of M_w/M_n and the chromatogram, and the monomer concentration dependence of the chromatograms became remarkable.

There are two significant differences between the experimental and theoretical ones for the samples prepared by solution polymerization, as stated in the previous section: The first is that the shift of the peak for the dimer should be caused by a decrease of $\langle S^2 \rangle$ due to the formation of a ring structure. The formation of a loop is not considered in Flory–Stockmayer theory, and, as is well-known, the crosslinking reaction in a dilute solution is susceptible to the formation of a ring structure. Actually, a shift of the peak for the dimer was observed for samples prepared in the dilute system (0.05 or 0.20 g ml^{-1}), while the location of peak of the dimer for F4-6 prepared by bulk polymerization is identical with that for the theoretical curve. This result indicates that the ring structure is formed in a dilute system.

The second is that the long-tailed distribution in the large $\langle S^2 \rangle$ region for the experimental traces would be due to the inequality in the reactivity of functional groups of the crosslinker. A schematic representation of the four types of reacted tetrafunctional crosslinkers is presented in Fig. 8. The reactivity of the third and fourth functional groups in the crosslinker should be much lower, because of the steric hindrance, than that of the first and second ones. On the other hand, the theory assumes an equal reactivity for all of the functional groups. Accordingly, the amount of crosslinkers with the Type-2 structure is expected to be greater, which

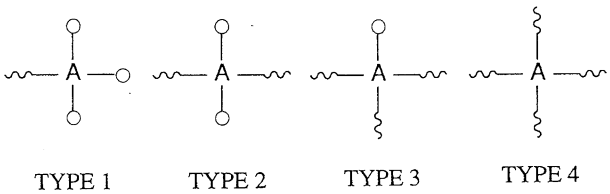

Fig. 8. Schematic representation for four types of the reacted tetrafunctional crosslinker.

gives rise to a less branched, more linear structure than that predicted by theory. This consideration is based on the assumption that the linear polymer has a larger $\langle S^2 \rangle$ than the branched polymer with identical molecular weight.[30] In order to verify this consideration, we performed two types of simulations (designated as RG3 and RG2), considering the two extreme cases for the reactivity of functional groups in the crosslinker: (RG3) the reactivity for one of four functional groups in the crosslinker is reduced to zero until p reaches 0.75, meaning that the crosslinker acts in a trifunctional way; (RG2) the reactivity for two of four groups is reduced to zero until p reaches 0.50, meaning that the crosslinker acts in a bifunctional way. The results for RG3 and RG2 are presented with the chromatogram of F4-6 at p=0.455 in Figs. 9a and 9b, respectively. The parameters used in the simulation are as follows: r=0.75, p=0.667 for RG3; r=0.50, p=1.0 for RG2. The result for RG3 is almost identical with that for the simulation which imposes no restrictions on the reactivity (RG4), suggesting that the contribution of the fourth group to the crosslinking reaction is quite small, even in a simulation assuming equal reactivity. Although the curve for RG2 has a different shape from those for RG3 and RG4, the tailed distribution in the large $\langle S^2 \rangle$ region in experiments remains undescribed. The failure to describe the experimental results by RG3 and RG2 suggests that the reactivity of the functional groups decreases along with the process of hydrosilylation, and that the pre-gel system has a structure in which only clusters with a specific structure are linearly linked. This structure would be formed by the following process: The branching reaction proceeds mainly at low conversion; beyond a certain critical conversion the linear linking reaction between branched clusters is advanced due to a steric hindrance. Dusek et al.[31] also reported that the parts unable to join the reaction because of this steric hindrance appears in the precursor network along with the process of crosslinking. The post-gel, which is a combination of precursor networks with the structure stated above, is likely to have a spacial inhomogenity in its structure. Horie et al.[32] also proposed a heterogeneous post-gel structure in which the microgels created by heterogeneous polymerization at the first reaction stage are connected with one another for the crosslinked copolymerization of methyl methacrylate with ethylene dimethacrylate. Recent small angle neutron scattering studies[33,34] concerning the post-gel structure also suggest that the crosslinking procedure gives rise to spacial heterogenity in the post-gel system.

The chromatograms of F4-7 and F4-8 with $r \neq 1$ shown in Figs. 5a and 5b have different shapes from those of samples with r=1. However, the differences between the experimental and theoretical curves, namely, the peak shift of the dimer and the tailed distribution in the large $\langle S^2 \rangle$ region, are the same as those for samples with r=1, suggesting that the samples with different r values have similar structural features, as described above.

Hydrosilylation between Bifunctional Monomer and a Trifunctional Crosslinker. In Figs. 6a and 6b, the features in the comparison of the experimental traces with the theoretical ones are governed by whether the sample is prepared in a dilute or bulk system, similarly to the F4-x series. It should be noticed in Fig. 6b that the amount of the unreacted monomer is large, and that of unreacted crosslinker is small compared with those predicted by theory, implying that the degree of crosslinking involved in clusters more than dimer is greater than the theoretical one. We estimated the molar ratio of the monomer to the crosslinker involved in clusters more than dimer as follows: The molar concentrations of the monomer and crosslinker in clusters at conversion p ($[M]_{p-0}$ and $[C]_{p-0}$, respectively) are respectively given by

$$[M]_{p-0} = [M]_0 - \frac{[M]_p[T]_0}{[T]_p} \quad (4)$$

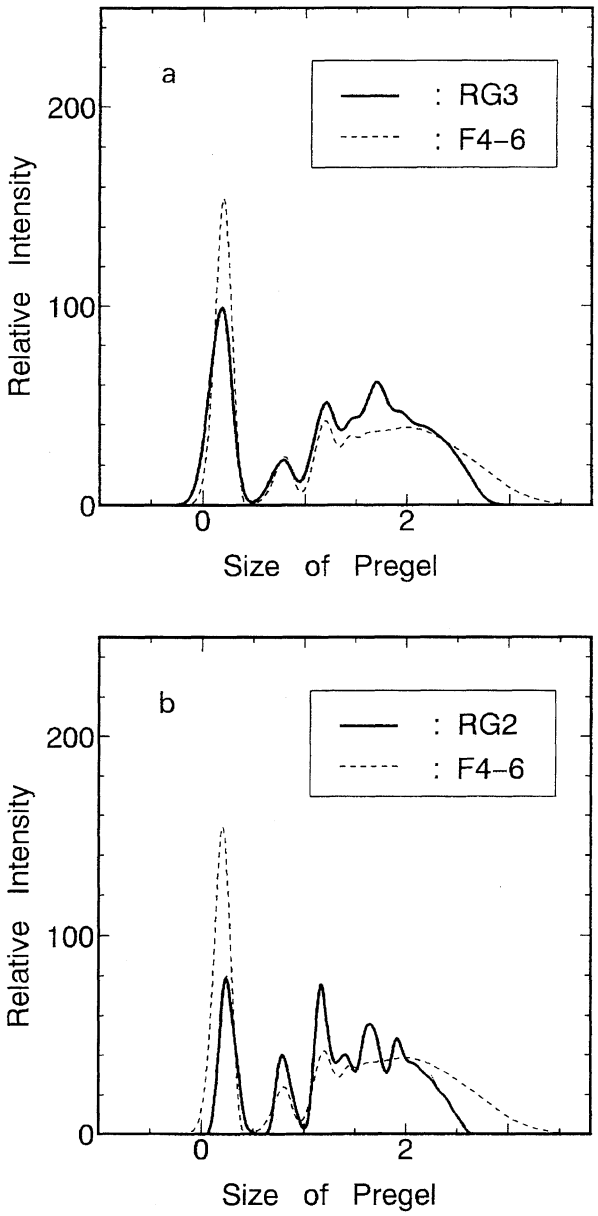

Fig. 9. (a) Comparison of the GPC curve of F4-6 at p=0.455 with the curve calculated by RG3. (b) Comparison of the GPC curve of F4-6 at p=0.455 with the curve calculated by RG2.

and

$$[C]_{p-0} = [C]_0 - \frac{[C]_p[T]_0}{[T]_p}, \quad (5)$$

where $[M]_0$ and $[C]_0$ are, respectively, the initial concentration of the monomer and crosslinker, and $[M]_p$ and $[C]_p$ are the concentrations of the unreacted monomer and crosslinker at p, respectively. $[T]_0$ and $[T]_p$ are the concentrations of toluene used as the standard at $p=0$ and p, respectively. Each concentration was determined based on the peak area corresponding to each component. Using Eqs. 4 and 5, the experimental and theoretical values of $[M]_{p-0}/[C]_{p-0}$ were estimated to be 1.16 and 1.24, respectively. The smaller value of $[M]_{p-0}/[C]_{p-0}$ for the experiment suggests that the degree of the crosslinker used in hydrosilylation is greater than that predicted by theory. The excess of the crosslinker would contribute to the linear linking reaction in the formation of the network structure mentioned before.

Hydrosilylation between Bifunctional Monomers. Since the branching reaction does not occur in this case, the $\langle S^2 \rangle$ distribution can be directly related to the molecular weight distribution, differing from the case in which the functionality of the crosslinker is more than three. The GPC trace of F2-1 is shifted to the left in the large $\langle S^2 \rangle$ region compared with the theoretical one, as shown in Fig. 7a. On the other hand, the chromatogram of F2-2 agrees well with the theoretical one, as indicated in Fig. 7b. The shift observed in Fig. 7a can be explained by the formation of a ring structure. In the case of $r=1$ (F2-1), the probability that both ends of a cluster consist of one Si–H group and one vinyl group is not small, which leads to an increase in the chance of a coupling reaction between both ends. On the other hand, in the case of $r=2$ (F2-2), the formation of a ring structure should hardly occur, because most of clusters have an Si–H group at both ends.

Conclusions

The size distribution of polymer clusters in the pre-gel state was investigated as a function of the conversion by GPC with varying the functionality of the crosslinker and synthetic conditions. The size distribution of polymer clusters at low conversion was independent of the synthetic conditions, such as the reaction temperature, catalyst concentration, and monomer concentration. The GPC chromatograms at low conversion were well described by a theoretical one based on the $\langle S^2 \rangle$ distribution predicted by the Flory–Stockmayer theory and the Gaussian chain statistics. The size distribution at high conversion depended only on the monomer concentration. The formation of the ring structure was supposed in a system prepared at low concentration. The experimental GPC traces at high conversion had a long tailed shape in the large $\langle S^2 \rangle$ region, compared with the theoretical one. The molar ratio of the crosslinker to the monomer consumed on hydrosilylation at high conversion was found to be greater than the theoretical value. We deduced the process of gel formation and the post-gel structure from the results obtained in this study. The branching reaction proceeds as predicted by theory at low conversion. With increasing conversion, the amount of the crosslinker contributing to the linear linking reaction between the branched clusters increases due to the steric hindrance around the functional groups. This process gives rise to the more linear structure than the theoretical description. The post-gel, which is formed by the association of precursor networks with the structure stated above, is expected to have spacial inhomogeneity in its structure.

References

1) R. S. Whitney and W. Burchard, *Makromol. Chem.*, **181**, 869 (1980).
2) M. Daoud, F. Family, and G. Jannink, *J. Phys. Lett. (Paris)*, **45**, L199 (1984).
3) M. Adam, M. Delsanti, J. P. Munch, and D. Durand, *J. Phys. Lett. (Paris)*, **48**, 1809 (1987).
4) M. Adam, M. Delsanti, R. Okasha, and G. Hild, *J. Phys. Lett. (Paris)*, **40**, L539 (1979).
5) D. F. Hodgson and E. J. Amis, *Macromolecules*, **23**, 2512 (1990).
6) J. C. Scanlan and H. H. Winter, *Macromolecules*, **24**, 47 (1991).
7) P. J. Flory, "Principles of Polymer Chemistry," Cornell University Press, Ithaca, New York (1953).
8) W. Stockmayer, *J. Chem. Phys.*, **11**, 45 (1943).
9) W. Stockmayer, *J. Chem. Phys.*, **12**, 125 (1944).
10) D. Stauffer, A. Coniglio, and M. Adam, *Adv. Polym. Sci.*, **44**, 103 (1982).
11) D. Stauffer, "Introduction to Percolation Theory," Taylor & Francis, London (1985).
12) P.-G. de Gennes, "Scaling Concepts in Polymer Physics," Cornell University Press, Ithaca, New York (1979).
13) F. Schosseler, H. Benoit, Z. Grubisic-Gallot, C. Strazielle, and L. Leibler, *Macromolecules*, **22**, 400 (1989).
14) A. Kidera and S. Kohjiya, *Comp. Polym. Sci.*, **2**, 72 (1992).
15) H. A. Kramers, *J. Chem. Phys.*, **14**, 415 (1946).
16) G. R. Dobson and M. J. Gordon, *J. Chem. Phys.*, **41**, 2389 (1964).
17) M. A. Llorente and J. E. Mark, *Macromolecules*, **13**, 681 (1980).
18) M. Gotttlieb, C. W. Macosko, G. S. Benjamin, K. O. Meyers, and E. W. Merril, *Macromolecules*, **14**, 1039 (1981).
19) E. M. Valles, E. J. Rost, and C. W. Macosko, *Rubber Chem. Technol.*, **57**, 55 (1984).
20) W. Opperman and N. Rennar, *Prog. Colloid Polym. Sci.*, **75**, 49 (1987).
21) S. K. Patel, S. Malone, C. Cohen, J. R. Gillmor, and R. H. Colby, *Macromolecules*, **25**, 5241 (1992).
22) S. Mallam, A.-M. Hecht, E. Geissler, and P. Pruvost, *J. Chem. Phys.*, **91**, 6447 (1989).
23) T. Ando, S. Yamanaka, S. Kohjiya, and K. Kajiwara, *Polym. Gels Networks*, **1**, 45 (1993).
24) H. Kazama, Y. Tezuka, and K. Imai, *Polym. Bull.*, **21**, 31 (1989).
25) J. L. Speier, *Adv. Organomet. Chem.*, **17**, 407 (1979).
26) S. Kohjiya, A. Ono, and S. Yamashita, *Polym.-Plast. Technol. Eng.*, **30**, 351 (1991).
27) W. Noll, "Chemistry and Technology of Silicone," Academic Press, New York (1968).
28) S. Kohjiya, K. Maeda, S. Yamashita, and Y. Shibata, *J. Mater. Sci.*, **25**, 3368 (1990).

29) L. H. Tung, *J. Appl. Polym. Sci.*, **10**, 375 (1966).
30) B. H. Zimm and W. H. Stockmayer, *J. Chem. Phys.*, **17**, 1301 (1949).
31) K. Dusek, "Developments in Polymerization-3," ed by R. N. Haeard, Appl. Sci. Pub., (1982).
32) K. Horie, A. Otagawa, M. Muraoka, and I. Mita, *J. Polym. Sci., Polym. Chem. Ed.*, **13**, 445 (1975).
33) J. Bastide, L. Leibler, and J. Prost, *Macromolecules*, **23**, 1821 (1990).
34) E. Mendes, P. Lindner, M. Buzier, F. Boué, and J. Bastide, *Phys. Rev. Lett.*, **66**, 1595 (1991).